AD-A130 665 SCATTERING OF WAVES BY IRREGULARITIES IN PERIODIC DISCRETE LATTICE SPACES..(U) LA JOLLA INST CA CENTER FOR THE STUDY OF NONLINEAR DYNAMICS.. 1/1

UNCLASSIFIED N POMPHREY ET AL. 1983 LJI-R-83-229 F/G 12/1 NL

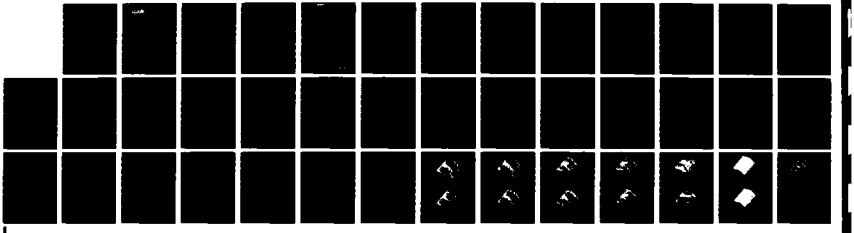

END

FILMED

DTIC

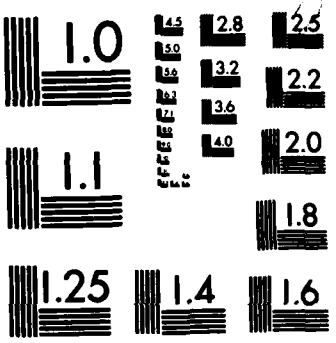

MICROCOPY RESOLUTION TEST CHART
NATIONAL BUREAU OF STANDARDS-1963-A

LaJolla INSTITUTE

CENTER FOR STUDIES OF NONLINEAR DYNAMICS
8950 VILLA LA JOLLA DRIVE • SUITE 2150
LA JOLLA • CALIFORNIA 92037 • PHONE (619) 454-3581

LJI-R-83-229

SCATTERING OF WAVES BY IRREGULARITIES IN PERIODIC DISCRETE LATTICE SPACES II. CALCULATIONS

by

Neil Pomphrey,
Elliott W. Montroll
and
Bruce J. West

Center for Studies of Nonlinear Dynamics*
La Jolla Institute
P.O. Box 1434
La Jolla, CA 92038

*Affiliated with University of California, San Diego

Supported by the Defense Advanced Research Projects Agency

LJI-R-83-229

SCATTERING OF WAVES BY IRREGULARITIES IN PERIODIC DISCRETE LATTICE SPACES
II. CALCULATIONS

by

Neil Pomphrey,
Elliott W. Montroll
and
Bruce J. West

Center for Studies of Nonlinear Dynamics*
La Jolla Institute
P.O. Box 1434
La Jolla, CA 92038

*Affiliated with University of California, San Diego

Supported by the Defense Advanced Research Projects Agency

TABLE OF CONTENTS

SECURITY CLASSIFICATION UNCLASSIFIED (When Data Entered)

REPORT DOCUMENTATION PAGE

READ INSTRUCTIONS BEFORE COMPLETING FORM

1. REPORT NUMBER AFOSR-TR- 83-0633	2. GOVT ACCESSION NO. AD-A132665
3. RECIPIENT'S CATALOG NUMBER	
4. TITLE (and Subtitle) Scattering of Waves by Irregularities in Periodic Discrete Lattice Spaces II. Calculations	5. TYPE OF REPORT & PERIOD COVERED 15 Aug 81 – 14 Feb 84 Interim Report
	6. PERFORMING ORG. REPORT NUMBER LJI-R-83-229
7. AUTHOR(s) Neil Pomphrey, Elliott W. Montroll and Bruce J. West	8. CONTRACT OR GRANT NUMBER(s) F49620-81-K-0017
9. PERFORMING ORGANIZATION NAME AND ADDRESS Center for Studies of Nonlinear Dynamics, La Jolla Institute, 8950 Villa La Jolla Drive, Suite 2150, La Jolla, California 92037	10. PROGRAM ELEMENT, PROJECT, TASK AREA & WORK UNIT NUMBERS 61102F 2306/A2
11. CONTROLLING OFFICE NAME AND ADDRESS Department of the Air Force Air Force Office of Scientific Research (AFOSR) Bolling Air Force Base, DC 20332	12. REPORT DATE 1983
	13. NUMBER OF PAGES 36
14. MONITORING AGENCY NAME & ADDRESS(if different from Controlling Office) [illegible]	15. SECURITY CLASS. (of this report) UNCLASSIFIED
	15a. DECLASSIFICATION/DOWNGRADING SCHEDULE

16. DISTRIBUTION STATEMENT (of this Report)

Approved for public release; distribution unlimited.

17. DISTRIBUTION STATEMENT (of the abstract entered in Block 20, if different from Report)

18. SUPPLEMENTARY NOTES

19. KEY WORDS (Continue on reverse side if necessary and identify by block number)

discrete scattering, exact model, asymmetric scatterers, lattice Greens functions

20. ABSTRACT (Continue on reverse side if necessary and identify by block number)

The general formalism for the exact scattering of a scalar wave from N scatterers on a discrete lattice is reviewed. The interpretation of the exact solution in terms of approximation techniques is given and the expression for the scattering cross sections is derived. The expressions necessary for the calculation of the lattice Greens function are discussed and a number of asymmetric scattering configurations are considered.

DD FORM 1 JAN 73 1473 EDITION OF 1 NOV 65 IS OBSOLETE

UNCLASSIFIED

SECURITY CLASSIFICATION OF THIS PAGE (When Data Entered)

1. INTRODUCTION

In this report we investigate the scattering of scalar waves from a distribution of a finite number of scatterers. The technique we employ was developed by Montroll and West[1] to describe the discrete scattering of scalar waves from defects on regular lattices. The method makes no assumptions about the symmetry of the scatterers and therefore can be applied to inhomogeneities of arbitrary shape. The majority of the approaches used in the past have had to either truncate the multiple scattering integrals at some appropriate order[2] or restrict the investigation to scatterers having a high degree of symmetry.[3] We avoid both these limitations here by characterizing a scatterer by a distribution of N defects and solving the scattering problem for these N defects *exactly*. The only limitation of the technique is the maximum number of defects one can use to specify the scatterer, which in turn is determined by limitations in computation time.

The problem posed by the scattering of a scalar wave from a fixed obstacle of known shape and composition is primarily numerical and involves the solution of a linear integral equation. The propagation of an ultrasonic wave through a homogeneous, isotropic elastic material is described by a scalar wave equation. The scattering of such a wave from an imperfection in the solid generates both longitudinal and transverse waves, which satisfy linear integral equations with a propagation kernel given by a Greens tensor.[4] At present a numerically tractable theory for the scattering of an elastic wave from a flaw of arbitrary shape, i.e. one not possessing spatial symmetry, does not exist. In nondestructive evaluation (NDE), where such waves are used as probes to determine the shape, size and composition of flaws in materials, the analysis has been restricted to either long or short wave approximations. In the former case the Born

approximation has been used extensively[5] and in the latter a generalization of the diffractive geometric optics approximation originally due to Keller[6] has been used. An approach which can span the gap in wavelengths between these two extremes is highly desirable.

Herein we limit our discussion to scalar waves scattering from inhomogeneities and examine properties of the scattered wavefield in the far field region. Among the scattering configurations we examine are line scatterers of finite length, i.e., hairline cracks, including the effects of bends in the crack and cracks of finite lateral extent also rectangular patches of scatterers. The exact scattered wavefield from such theoretically repelling, but physically interesting objects has not been calculated previously.

In Section 2 we review the mathematical formalism for the scattering of scalar waves from defects on a simple cubic lattice. The lattice is chosen for computational convenience and is not to be confused with the crystal lattice of the material. A real metal such as iron consists of an agglomeration of crystals having a characteristic dimension of 0.025 cm with arbitrary shapes and orientations. Each of these crystals is called a grain and there exists a distribution of grain sizes in such polycrystalline materials. The distribution of grain sizes determines the fracture micro-mechanics of the elastic material and can dominate such effects as crack formation and propagation. Here we are not concerned with the generation or evolution of cracks, but rather with their detection. Thus we feel that the use of our computational lattice is justified for this preliminary investigation of S-wave scattering in NDE. We show in Section 2 that in the solution for the scattering of a wave from N defects no assumptions are made about the relative positioning of the defects. An extended scattering object is therefore represented by a distribution of N such defects. The Montroll-West model solution is not an exact representation of the scattering

from a flaw, because the flaw is represented by only N defects. However, the ratio of determinants is the *exact* scattering solution to the N point representation of the flaw.[1] The exact nature of the model enables one to exploit the method to determine the effects of interference and resonance in the specular reflection from cracks.

In Section 3 we discuss the physical interpretation of the form of the solution to the N defect scattering problem. One can relate the terms in the expansion of the determinants to scattering diagrams and associate elements with particular multiple scattering effects. In this way various effects can be systematically suppressed by using approximations to the expanded form of the determinants. It is suggested that this technique can be used to check other approximation methods in situations where exact analytic or numerical calculations cannot be made using more standard methods.

In Section 4 we present the results of our calculations.

2. DISCRETE SCATTERING MODEL

A. Continuum Equations

The propagation of a scalar wave through a homogeneous, isotropic elastic material is described by the wave equation

$$\nabla^2 \psi(\mathbf{r},t) - \frac{1}{c^2} \frac{\partial^2}{\partial t^2} \psi(\mathbf{r},t) = 0 \qquad (2.1)$$

where $\psi(\mathbf{r},t)$ is the wavefield at position $\mathbf{r}$ and time t and c is the wave speed in the material. For a wavefield of frequency ω, i.e. $\psi(\mathbf{r},t) = \Phi(\mathbf{r}) \exp[-i\omega t]$, we can rewrite (2.1) as the Helmholtz equation

$$\frac{1}{2} \nabla^2 \Phi(\mathbf{r}) + n^2 k_0^2 \Phi(\mathbf{r}) = 0 \qquad (2.2)$$

where the factor of $\frac{1}{2}$ has been introduced for later convenience and $n^2 \equiv \omega^2 / 2c^2 k_0^2$. The Helmholtz equation is an elliptic partial differential equation, so that in order to find the field Φ at a given point $\mathbf{r}$ one must solve the equation for the field at all points in space. This property of elliptic partial differential equations severely limits the analytical and numerical tractability of (2.2).

The Helmholtz equation arises in many contexts, e.g. in the propagation of electromagnetic waves in media where polarization effects are not important; the Schrödinger description of a matter wave in an energy eigenstate, etc. Each of these applications has precipitated its own sequence of approximations for solving (2.2), including the conversion of (2.2) into a parabolic differential equation. The physically interesting situation is when the medium is non-homogeneous, e.g. flaws in an elastic material. In this case we write

$$n^2 = 1 + V(\mathbf{r}) / k_0^2 \qquad (2.3)$$

where $V(\mathbf{r})$ characterizes the inhomogeneity. This function can also be the potential in quantum mechanics, the variable index of refraction in a medium with changing optical properties, the spatially dependent dielectric coefficient

for a plasma with density variations, etc. The solution of (2.2) with (2.3) inserted is given by the integral equation

$$\Phi(\mathbf{r}) = \Phi_0(\mathbf{r}) - \int g(\mathbf{r},\mathbf{r}';n_0)\ V(\mathbf{r}')\ \Phi(\mathbf{r}')\, d^3r' \tag{2.4}$$

where $g(\mathbf{r},\mathbf{r}';n_0)$ is the Greens function that satisfies the equation

$$\frac{e}{2}\nabla^2 g(\mathbf{r},\mathbf{r}';n_0) + k_0^2\, g(\mathbf{r},\mathbf{r}';n_0) = \delta(\mathbf{r}-\mathbf{r}'), \tag{2.5}$$

and $\Phi_0(\mathbf{r})$ is the wavefield when $V(\mathbf{r}) = 0$.

B. Discrete Equations

The discrete analog of the Helmholtz equation is here obtained by interpreting the ∇^2 in (2.1) as the second difference "Laplacian"

$$\nabla^2 \equiv \frac{1}{b^2}\sum_{j=1}^{3}\left(E_j - 2 + E_j^{-1}\right) \tag{2.6}$$

where the $E_j^{\pm 1}$'s are the discrete translation operators on a simple cubic lattice, i.e.

$$f(l_1,\cdots l_j\cdots l_n) = E_j\, f(l_1,\cdots l_j - 1\cdots l_n)$$

$$= E_j^{-1}\, f(l_1\cdots l_j + 1\cdots l_n). \tag{2.7}$$

The position vector $\mathbf{r} = \mathbf{l}\,b$ has the lattice components (l_1,l_2,l_3) with the elements of $\mathbf{l}$ being integers and b is the lattice spacing. The free lattice can support the propagation of plane waves with frequency ω and wave vector $\mathbf{k} = (k_1,k_2,k_3)$ so we substitute the plane wave

$$\Phi_0(\mathbf{l}\,b) = \exp\{i\,\mathbf{k}\cdot\mathbf{l}\,b\} \tag{2.8}$$

into (2.2) and replace $n^2k_0^2$ by the eigenvalues $\lambda_{\mathbf{k}}$, i.e.

$$\lambda_{\mathbf{k}} = \frac{1}{b^2}[\,3 - \cos(bk_1) - \cos(bk_2) - \cos(bk_3)]. \tag{2.9}$$

We impose periodic boundary conditions on the lattice such that $\Phi(x+Nb,y,z) = \Phi(x,y+Nb,z) = \Phi(x,y,z+Nb) = \Phi(x,y,z)$. This imposition restricts the components of $\mathbf{k}$ to integral multiples of 2π / Nb, i.e., $\mathbf{k} = \frac{2\pi}{Nb}\mathbf{n}$ where $\mathbf{n} \equiv (n_1,n_2,n_3)$ and $\{n_1,n_2,n_3\} = 0,1,\cdots N$. Introducing the

lattice Greens function

$$G(\mathbf{l}\,b;n_0) = \frac{1}{N^3}\sum_{\mathbf{n}} A_{\mathbf{n}} \exp\{i\,\frac{2\pi}{N}\mathbf{n}\cdot\mathbf{l}\} \tag{2.10}$$

into the discrete analog of (2.5) and equating coefficients of exp {i 2π n . l / N }, yields $A_{\mathbf{n}} = (n_0^2 - \lambda_{\mathbf{k}})^{-1}$. Thus the Greens function on the simple cubic lattice is given by

$$G(\mathbf{l}b\,;n_0) = \frac{b^2}{N^3} \sum_{n_1,n_2,n_3 = 1}^{N} \frac{\exp\{i2\pi\,\mathbf{n}\cdot\mathbf{l}/N\}}{\left[k_0^2\,b^2 - 3\right] + \sum_{j=1}^{3}\cos(2\pi n_j/N)} \tag{2.11}$$

when there are N lattice sites in each of the three dimensions. The Greens function (2.11) describes the free propagation of a plane wave on a homogeneous isotropic simple cubic lattice.

C. "Potential" Scattering

We consider a set of time independent defects on the set of lattice points $\{\mathbf{l}_\alpha\}$, $\alpha = 1, 2 \ldots, n$. In the presence of these defects the discrete Helmholtz equation takes on the inhomogeneous form

$$\left[\frac{1}{2}\Delta^2 + k_0^2\right]\Phi(\mathbf{l}\,b) = -\lambda\,V(\mathbf{l})\,\Phi(\mathbf{l}\,b) \tag{2.12}$$

where

$$V(\mathbf{l}) = \begin{cases} k_0^2 & \mathbf{l} = \{\mathbf{l}_\alpha\} \\ 0 & \textit{otherwise} \end{cases} \tag{2.13}$$

and $\lambda\,(\equiv \frac{\delta\rho}{\rho_0})$ is the strength of the defect, here produced by a variation in the density at the set of sites $\{\mathbf{l}_\alpha\}$. We shall refer to V (l) as the scattering potential for the wave and λ as its strength. The plane wave (2.8) is a solution to (2.12)

in the limit $\lambda \to 0$. The full solution of the inhomogeneous equation (2.12) is then a linear superposition of the incident plane wave and the scattered wave produced by the potential, i.e.

$$\Phi(\mathbf{l}b) = \exp\{i\mathbf{k}_i \cdot \mathbf{l}b\} - \lambda \sum_{a=1}^{N} G(\mathbf{l} - \mathbf{l}_a; n_0)\ V(\mathbf{l}_a)\,\Phi(\mathbf{l}_a b) \quad (2.14)$$

which is analogous to the continuum solution (2.4). We have indicated the value of the incident wave vector by $\mathbf{k}_i$ in (2.14).

To solve equation (2.14) for the total wave field $\Phi(\mathbf{l}\,b)$ we introduce the notation

$$G_{\alpha\beta} \equiv G(\mathbf{l}_\alpha - \mathbf{l}_\beta; n_0);\ G_{0\alpha} \equiv G(\mathbf{l} - \mathbf{l}_\alpha; n_0);\ \Phi_\alpha \equiv \Phi(\mathbf{l}_\alpha b)$$

and

$$V_\alpha \equiv V(\mathbf{l}_\alpha). \quad (2.15)$$

Then if we successively let $\mathbf{l}$ be equal to the location of each of the n potential sites $\{\mathbf{l}_\alpha\}$ in (2.14) we obtain the n inhomogeneous linear equations

$$\begin{aligned}
(1 + \lambda G_{11} V_1)\,\Phi_1 + \lambda\, G_{12}\, V_2 \Phi_2 \cdots\cdots + \lambda\, G_{1n}\, V_n\, \Phi_2 &= \exp\{i\mathbf{k}_i \cdot \mathbf{l}_1 b\} \\
\lambda\, G_{21}\, V_1 \Phi_1 + (1 + \lambda\, G_{22}\, V_2)\,\Phi_2 \cdots\cdots + \lambda\, G_{2n}\, V_n\, \Phi_n &= \exp\{i\mathbf{k}_i \cdot \mathbf{l}_2 b\} \\
&\ \ \vdots \qquad\qquad\qquad\qquad\qquad\qquad\ \ \vdots \\
\lambda\, G_{n1}\, V_1\, \Phi_1 + \lambda\, G_{n2}\, V_2\, \Phi_2 \cdots + (1 + \lambda G_{nn} V_n)\Phi_n &= \exp\{i\mathbf{k}_i \cdot \mathbf{l}_n b\}\ .
\end{aligned}$$

The solution to this set of equations when n=2 is

$$\Phi_1 = \frac{1}{\Delta_2} \begin{bmatrix} \exp(i\mathbf{k}_i \cdot \mathbf{l}_1 b) & \lambda\, G_{12}\, V_2 \\ \exp(i\mathbf{k}_i \cdot \mathbf{l}_2 b) & 1 + \lambda\, G_{22}\, V_2 \end{bmatrix} \quad (2.17a)$$

$$\Phi_2 = \frac{1}{\Delta_2} \begin{bmatrix} 1 + \lambda\, G_{11}\, V_1 & \exp(i\mathbf{k}_i \cdot \mathbf{l}_1 b) \\ \lambda\, G_{21}\, V_1 & \exp(i\mathbf{k}_i \cdot \mathbf{l}_2 b) \end{bmatrix} \quad (2.17b)$$

where

$$\Delta_2 \equiv \begin{bmatrix} 1 + \lambda G_{11} V_1 & \lambda G_{12} V_2 \\ \lambda G_{21} V_1 & 1 + \lambda G_{22} V_2 \end{bmatrix} . \qquad (2.17c)$$

When (2.17a) and (2.17b) are introduced into the solution (2.14), the full expression for $\Phi(\mathbf{1}b)$ becomes a sum of terms which is easily arranged as the ratio of two determinants. The total wavefield at the observation site $\mathbf{1}$ is then given by

$$\Phi(\mathbf{1}b) = \frac{1}{\Delta_2} \begin{bmatrix} \exp(i\,\mathbf{k}_i \cdot \mathbf{1}b) & \lambda G_{01} V_1 & \lambda G_{02} V_2 \\ \exp(i\,\mathbf{k}_i \cdot \mathbf{l}_1 b) & 1 + \lambda G_{11} V_1 & \lambda G_{12} V_2 \\ \exp(i\,\mathbf{k}_i \cdot \mathbf{l}_2 b) & \lambda G_{21} V_1 & 1 + \lambda G_{22} V_2 \end{bmatrix} \qquad (2.18)$$

The above argument may be repeated in every detail to obtain the total wavefield after scattering from n point potentials:

$$\Phi(\mathbf{1}b) = \frac{1}{\Delta_n} \begin{bmatrix} \exp(i\,\mathbf{k}_i \cdot \mathbf{1}b) & \lambda G_{01} V_1 \cdots & \lambda G_{0n} V_n \\ \exp(i\,\mathbf{k}_i \cdot \mathbf{l}_1 b) & 1 + \lambda G_{11} V_1 & \lambda G_{1n} V_n \\ \vdots & & \vdots \\ \exp(i\,\mathbf{k}_i \cdot \mathbf{l}_n b) & \lambda G_{n1} V_1 \cdots & 1 + \lambda G_{nn} V_n \end{bmatrix} \qquad (2.19)$$

where

$$\Delta_n \equiv \det|\delta_{\alpha\beta} + \lambda G_{\alpha\beta} V_\beta|;\ \alpha,\beta = 1,2,\cdots n . \qquad (2.20)$$

We define the function $D_1(1,2,\cdots n)$ by the determinant

$$D_1(1,2,\cdots n) \equiv \begin{bmatrix} \exp(i\,\mathbf{k}_i \cdot \mathbf{l}_1 b) & \lambda G_{12} V_2 \cdots & \lambda G_{1n} V_n \\ \vdots & 1 + \lambda G_{22} V_2 & \vdots \\ \exp(i\,\mathbf{k}_i \cdot \mathbf{l}_n b) & \cdots & 1 + \lambda G_{22} V_n \end{bmatrix} \qquad (2.21)$$

and are therefore able to express the wavefield at the site $\mathbf{l}_1$ as

$$\Phi(\mathbf{l}_1 b) = D_1(1,2,\cdots n)/\Delta_n . \qquad (2.22)$$

At the arbitrary potential site $\mathbf{l}_\beta$ we can write the wavefield as

$$\Phi(\mathbf{l}_\beta b) = D_\beta(\beta,\beta+1,\ldots n,\cdots \beta-1)/\Delta_n \qquad (2.23)$$

where the ordering of the indices in the determinant D_β is just a cyclic permutation of the lattice site indices in (2.21). The exact total wavefield can then be written as

$$\Phi(\mathbf{l}\,b) = \exp\{i\,\mathbf{k}_i \cdot \mathbf{l}\,b\} - \frac{\lambda}{\Delta_n} \sum_{a=1}^{n} G_{0a}\, V_a\, D_a \qquad (2.24)$$

which is an expansion of the determinant solution (2.19) in terms of minors.

3. INTERPRETATION OF EXACT SOLUTION

In this section we investigate expressions for the scattered wavefield as sums of contributions from single scattering, double scattering, triple scattering etc. The series we obtain are analogous to the Born series, but the individual propagators are renormalized, i.e. they contain factors that correspond to the resummation of interaction terms of a particular form. Let us first examine various choices for these resummations.

A. Renormalized Potentials and Propagators

Consider the following factored form for the determinant Δ_n:

$$\Delta_n \equiv (1 + \lambda G_{11} V_1)(1 + \lambda G_{22} V_2) \cdots \tilde{\Delta}_n \tag{3.1}$$

where we define the scaled determinant

$$\tilde{\Delta}_n \equiv \det| \delta_{\alpha\beta} + (1 - \delta_{\alpha\beta}) \lambda G_{\alpha\beta} \tilde{V}_\beta | \; ; \alpha,\beta = 1, 2, \cdots n \tag{3.2}$$

and $\tilde{V}_\beta$ is to be interpreted as the renormalized potential

$$\tilde{V}_\beta \equiv V_\beta (1 + \lambda G_{\beta\beta} V_\beta)^{-1} . \tag{3.3}$$

In terms of $\tilde{\Delta}_n$ and $\tilde{V}_\beta$ the wavefield (2.19) can be expressed as

$$\Phi(\mathbf{l}\, b) = \frac{1}{\tilde{\Delta}_n} \begin{bmatrix} \exp(i\, \mathbf{k}_i \cdot \mathbf{l}\, b) & \lambda G_{01} \tilde{V}_1 \cdots & \lambda G_{0n} \tilde{V}_n \\ \exp(i\, \mathbf{k}_i \cdot \mathbf{l}_1\, b) & 1 & \lambda G_{1n} \tilde{V}_n \\ \vdots & & \vdots \\ \exp(i\, \mathbf{k}_i \cdot \mathbf{l}_n\, b) & \lambda G_{n1} \tilde{V}_1 \cdots & 1 \end{bmatrix} . \tag{3.4}$$

Each off-diagonal element of the determinant (3.4) has the form

$$\lambda G_{\alpha\beta} \tilde{V}_\beta = \frac{\lambda G_{\alpha\beta} V_\beta}{1 + \lambda G_{\beta\beta} V_\beta} = \lambda G_{\alpha\beta} V_\beta - \lambda^2 G_{\alpha\beta} V_\beta G_{\beta\beta} V_\beta + O(\lambda^3) . \tag{3.5}$$

which corresponds to a self-interaction term in a diagrammatic expansion. Such resummations are mandatory when considering scattering from potentials

whose strength becomes singular at short distances, e.g. nuclear scattering, hard spheres collisions or specular reflections of scalar waves from caustics. It is clear that as $\lambda V_\beta \to \infty$ each terms on the right hand side of (3.5) diverges, whereas the infinite series converges to $G_{\alpha\beta} / G_{\beta\beta}$. Thus all the terms in the wavefield (3.4) are expressed in terms of the renormalized potentials so that each term individually remains finite as $\lambda V_\beta \to \infty$, i.e. $\lim_{\lambda V_\beta \to \infty} \lambda \tilde{V}_\beta = 1/G_{\beta\beta}$.

In the second renormalized form the determinant Δ_n is written in the factored form

$$\Delta_n = (1 + \lambda G_{11} V_1)\ (1 + \lambda G_{22} V_2) \cdots \tilde{\tilde{\Delta}}_n \tag{3.6}$$

where we define the scaled determinant $\tilde{\tilde{\Delta}}_n$ as

$$\tilde{\tilde{\Delta}}_n \equiv \det | \delta_{\alpha\beta} + (1 - \delta_{\alpha\beta}) \lambda\ \tilde{G}_{\alpha\beta} V_\beta | \ ;\alpha,\beta = 1,2, \cdots n \tag{3.7}$$

and $\tilde{G}_{\alpha\beta}$ is to be interpreted as the renormalized propagator

$$\tilde{G}_{\alpha\beta} \equiv G_{\alpha\beta} (1 + \lambda G_{\alpha\alpha} V_\alpha)^{-\frac{1}{2}} (1 + \lambda G_{\beta\beta} V_\beta)^{-\frac{1}{2}}. \tag{3.8}$$

Again we note that $\lambda \tilde{G}_{\alpha\beta} V_\beta$ remains finite as the set of potentials $\{ V_\alpha \}$ become infinite (as long as they all become infinite in the same way).

In terms of $\tilde{\tilde{\Delta}}_n$ and $\tilde{G}_{\alpha\beta}$ the total wavefield can be written as

$$\Phi(1b) = \frac{1}{\tilde{\tilde{\Delta}}_n} \begin{vmatrix} \exp(i \mathbf{k}_1 \cdot 1b) & U_1 \cdots & U_n \\ W_1 & 1 & \lambda \tilde{G}_{1n} U_n \\ \vdots & & \vdots \\ W_n & \lambda \tilde{G}_{n1} U_1 & \cdots 1 \end{vmatrix} \tag{3.10}$$

where we have introduced the functions.

$$U_\alpha = \lambda G_{0\alpha} V_\alpha / (1 + \lambda G_{\alpha\alpha} V_\alpha)^{\frac{1}{2}}. \tag{3.11a}$$

$$W_\alpha = \exp(i \mathbf{k}_i \cdot \mathbf{1}_\alpha b) / (1 + \lambda G_{\alpha\alpha} V_\alpha)^{\frac{1}{2}}. \tag{3.11b}$$

In this factorization, an expansion of the determinant (3.10) in minors always yields terms of the form $U_\alpha W_\alpha$ which remain finite for singular potentials. The renormalization Greens functions in (3.10) can be interpreted as the propagation of a plane wave on a lattice distorted by the presence of the n point-potentials.

B. Multiple Scattering Approximations

Consider first the case of plane wave scattering from three point potentials, $\{\mathbf{l}_\alpha\} = \mathbf{l}_1, \mathbf{l}_2, \mathbf{l}_3$. The solution (3.4) can be expressed in terms of:

$$g_{\alpha\beta} \equiv \lambda\, G_{\alpha\beta}\, \tilde{V}_\beta \tag{3.12}$$

as

$$\Phi(\mathbf{l}b) = \frac{1}{\tilde{\Delta}_3} \begin{vmatrix} \exp(i\,\mathbf{k}_i \cdot \mathbf{l}b) & g_{01} & g_{02} & g_{03} \\ \exp(i\,\mathbf{k}_i \cdot \mathbf{l}_1 b) & 1 & g_{12} & g_{13} \\ \exp(i\,\mathbf{k}_i \cdot \mathbf{l}_2 b) & g_{21} & 1 & g_{23} \\ \exp(i\,\mathbf{k}_i \cdot \mathbf{l}_3 b) & g_{31} & g_{32} & 1 \end{vmatrix} . \tag{3.13}$$

Expanding the determinant in the numerator of (3.13) yields

$$\Phi(\mathbf{l}b) = e^{i\mathbf{k}_i \cdot \mathbf{l}b} + \frac{1}{\tilde{\Delta}_3} \sum_{\alpha=1}^{3} g_{0\alpha}\, e^{i\mathbf{k}_i \cdot \mathbf{l}_\alpha b} \left\{ \tilde{\Delta}_2(\bar{\alpha}) + \sum_{\beta \neq \alpha} g_{\alpha\beta} + \sum_{\beta \neq \gamma} g_{\beta\gamma} g_{\gamma\alpha} \right\} \tag{3.14}$$

The quantity $\tilde{\Delta}_2(\bar{1})$ is the 2 x 2 determinant $\tilde{\Delta}_2$ which involves only the g's with subscripts 2 and 3 but not 1. Each term in the expansion can be identified with a scattering diagram, [cf. Figure 1]. Figure 1a represents the single scattering of our original plane wave by the potential at site $\mathbf{l}_1$. The full form of the contribution of that term to $\Phi(\mathbf{l}b)$ is

$$g_{01} \frac{\tilde{\Delta}_2(\bar{1})}{\tilde{\Delta}_3} e^{i\mathbf{k}_i \cdot \mathbf{l}_1 b} = \lambda\, G_{01}\, \tilde{V}_1\, e^{i\mathbf{k}_i \cdot \mathbf{l}_1 b} \frac{\tilde{\Delta}_2(\bar{1})}{\tilde{\Delta}_3} . \tag{3.15}$$

The factor $\exp(i\,\mathbf{k}_i \cdot \mathbf{l}_1 b)$ in (3.15) represents the plane wave incident upon the scattering point $\mathbf{l}_1$; $\lambda\tilde{V}_1$ represents the effective (renormalized) scattering

potential and G_{01} corresponds to the scattered wave which propagates from $\mathbf{l}_1$ to the observer at $\mathbf{l}$. The ratio of the Δ's is the contribution of the other scattering points to the single scattered amplitude even though they are not directly involved in the scattering. They give rise to the distortion of the underling lattice very much like a mean field in which the single scattering occurs. As $\lambda \to 0$, $\tilde{V}_1 \to V_1$ [cf. (3.3)] and the ratio of the Δ's approaches unity so that (3.15) becomes a contribution to the first Born approximation of the solution in this limit.

In Figure 1b the diagram corresponding to the double scattering term

$$\tilde{\Delta}_3^{-1} g_{03} g_{31} \exp\{i \mathbf{k}_i \cdot \mathbf{l}_1 b\} \tag{3.16}$$

is depicted. Interpreting the factors in (3.16) from right to left, we have, the plane wave incident on lattice site $\mathbf{l}_1$, the scattering from $\mathbf{l}_1$ to $\mathbf{l}_3$ followed by the scattering from $\mathbf{l}_3$ to the observer at $\mathbf{l}$. The influence of those points not directly involved in the scattering is $\tilde{\Delta}_1(\bar{1},\bar{3})/\tilde{\Delta}_3$, but since $\tilde{\Delta}_1 = 1$, only the $\tilde{\Delta}_3$ factor appears.

These results are immediately generalized to the case of $m-th$ order scattering in a system of n scattering centers. The contribution to $\Phi(\mathbf{l}b)$ of the scattering sequence $\mathbf{l}_1 \to \mathbf{l}_{a_{m-1}} \to \cdots \mathbf{l}_{a_1} \to$ observer is

$$g_{0a_1} g_{a_1 a_2} \cdots g_{a_{m-2} a_{m-1}} g_{a_{m-1},1} e^{i \mathbf{k}_i \cdot \mathbf{l}_1 a} \tilde{\Delta}_{n-m}(\bar{\alpha}_1, \bar{\alpha}_2, \cdots, \bar{\alpha}_{m-1}, \bar{1}) / \tilde{\Delta}_n \tag{3.17}$$

where we let $\tilde{\Delta}_{n-m}(\bar{\alpha}_1, \bar{\alpha}_2, \cdots, \bar{\alpha}_{m-1}, 1)$ represent the determinant $\tilde{\Delta}_{n-m}$ which involves the (n-m) points not including the points from which the wave has been

scattered. Hence the field observed at site 1 can be expressed in the series form

$$\Phi(1b) = \exp\{i\,\mathbf{k}_i \cdot 1b\} + \sum_{a=1}^{n} g_{0a}\, e^{i\mathbf{k}_i \cdot 1_a b}\, \tilde{\Delta}_{n-1}(\bar{\alpha}) / \tilde{\Delta}_n$$

$$+ \sum_{a,\beta=1}^{n} g_{0a} g_{a\beta}\, e^{i\mathbf{k}_i \cdot 1_a \beta}\, \tilde{\Delta}_{n-2}(\bar{\alpha}, \bar{\beta}) / \tilde{\Delta}_n + \cdots \qquad (3.18)$$

This expansion is the generalization of the multiple Born expansion, but with all terms renormalized.

4. SCATTERING CROSS SECTION

As mentioned in the Introduction, the use of ultrasonic waves as a probe into the structure of materials has been very fruitful. In particular, measurements of the total power transmitted from source to receiver through an elastic material provides information on the distribution of scattering centers within that material. The attenuation of the ultrasonic wave in a distance z along its direction of propagation is $\exp[-\sigma(\omega)z]$ where the attenuation coefficient $\sigma(\omega)$ is dependent on the frequency of the incident wave and is proportional to the average cross section of the scatterers in the material. This relation has been used to determine the distribution of grain sizes in polycrystalline materials. If the attenuation of the wave is due primarily to the elastic scattering of energy out of the direction of propagation, then the elastic scattering cross section is a quantitative measure of how much the incident wave is attenuated along the straight line path joining the source and receiver. Even in the case of a localized scatterer such as a crack, the scattering cross section determines the intensity of the signal received at different observation points.

In the continuum the total wave field can be written as

$$\Phi(\mathbf{r}) = \exp\{i\,\mathbf{k}_i \cdot \mathbf{r}\} + \frac{\exp\{ikr\}}{r} f\,(\hat{\mathbf{k}}_i, \hat{\mathbf{k}}_f) \tag{4.1}$$

where the incident wave vector is $\mathbf{k}_i = \hat{\mathbf{k}}\,k_0$, the final wave vector is $\mathbf{k}_f = \hat{\mathbf{r}}k_0$ in terms of the unit vectors $\hat{\mathbf{k}} \equiv \mathbf{k}/k$, $\hat{\mathbf{r}} \equiv \mathbf{r}/r$. Here $\mathbf{r}$ is the asymptotic location of the observer; $f\,(\hat{\mathbf{k}}_i, \hat{\mathbf{k}}_f)$ is the amplitude of the scattered wave and $\cos^{-1}(\hat{\mathbf{k}}_i \cdot \hat{\mathbf{k}}_f) = \Theta$ is the scattering angle. The differential scattering cross section is given by

$$\frac{d\sigma}{d\Omega} = |f\,(\hat{\mathbf{k}}_i, \hat{\mathbf{k}}_f)|^2 \tag{4.2}$$

and the total scattering cross section is obtained by integrating (4.2) over the

solid angle $d\Omega = \sin\Theta\, d\Theta\, d\varphi$ i.e

$$\sigma_{tot} = 2\pi \int_0^{\pi} |f(\hat{\mathbf{k}}_i, \hat{\mathbf{k}}_f)|^2 \sin\Theta\, d\Theta \ . \tag{4.3}$$

The total wavefield on the lattice is given by (2.24) as

$$\Phi(\mathbf{l}b) = \exp\{i\,\mathbf{k}_i \cdot \mathbf{l}b\} - \frac{\lambda}{\Delta_n} \sum_{a=1}^{n} G_{0a}\, V_a\, D_a \ . \tag{4.4}$$

The scattered intensity is observed at $\mathbf{l}$ which is generally a considerable distance from a typical scattering site $\mathbf{l}_a$. Hence, the large $\mathbf{l}$ approximation can be used for G_{0a}. This is just the Greens function for the original continuum medium. The other G's in the determinant D_a are given by the appropriate lattice Greens functions [cf. (2.11)] determining the wave propagation among potential sites $\{\mathbf{l}_a\}$. We consider the limit of the lattice Greens function (2.11) as $N \to \infty$ and define the continuous variable $\lim_{n\to\infty} \frac{2\pi}{N} n_j = \varphi_j$ so that (2.11) becomes

$$G(\mathbf{l}b;n_0) = \frac{b^2}{(2\pi)^3} \int \int_{-\pi}^{\pi} \int \frac{\exp(i\,\mathbf{l}\cdot\varphi)\, d^3\varphi}{(k_0^2\, b^2 - 3) + \sum_{j=1}^{3} \cos\varphi_j} \ . \tag{4.5}$$

Now writing the continuum position $\mathbf{r} = \mathbf{l}b$ we can rewrite the lattice Greens function as

$$G(\mathbf{l}b;n_0) = b^3 G_0(\mathbf{r};k_0) \ . \tag{4.6}$$

The asymptotic form of the continuum Greens function is

$$G_0(\mathbf{r};k_0) = \frac{\exp\{ik_0 r\}}{4\pi r} \tag{4.7}$$

so that from (4.4) we obtain

$$\Phi(\mathbf{r}) = e^{i\mathbf{k}_i\cdot\mathbf{r}} - \frac{\lambda b^3}{4\pi\Delta_n} \sum_{a=1}^{n} \frac{e^{i\mathbf{k}_f\cdot(\mathbf{r}-\mathbf{r}_a)}}{|\mathbf{r}-\mathbf{r}_a|} V_a\, D_a \ . \tag{4.8}$$

Recall that $\mathbf{k}_f = k_0 \hat{\mathbf{r}}$ so that the amplitude of the scattered wavefield is

$$f(\hat{\mathbf{k}}_i, \hat{\mathbf{k}}_f) = -\frac{\lambda b^3}{4\pi\Delta_n} \sum_{a=1}^{n} e^{-ik_0 \hat{\mathbf{r}}\cdot\mathbf{r}_a} V_a D_a \qquad (4.9)$$

since $r \gg |\mathbf{r}_a|$. The dependence of the scattering amplitude on $\mathbf{k}_i$ is contained in D_a.

In a subsequent section we calculate $f(\hat{\mathbf{k}}_i, \hat{\mathbf{k}}_f)$ for various numbers and configurations of point scatterers.

5. CALCULATION OF LATTICE GREENS FUNCTION

It is clear from all our discussion that the scattering of waves off defects specified by V_a on a lattice is completely determined by the lattice Greens function. On a simple cubic lattice we rewrite (4.5) as

$$\mathcal{G}(\Omega;l,m,n) = \frac{1}{\pi^3}\int_0^\pi dx \int_0^\pi dy \int_0^\pi dz \ \frac{\cos lx \cos my \cos nz}{\Omega - \cos x - \cos y - \cos z} \qquad (5.1)$$

where the triad (l,m,n) specify the integer lattice coordinates, and $G = -b^2\,\mathcal{G}$. Because the integrand of (5.1) is both singular and oscillatory the numerical integration is non-trivial and requires a certain amount of discussion. There is a substantial literature on Greens functions of the form (5.1) since they arise in the model studies of many physical phenomena e.g. in the study of the distribution of magnetization around an impurity, i.e. localized spin wave modes and other problems in condensed matter physics.

The emphasis in the literature published on the numerical solutions of (5.1) has concentrated on obtaining accurate values of $\mathcal{G}(\Omega;0,0,0)$, i.e. the Greens function at the origin. For the purposes of scattering theory we need to do much better than this and obtain accurate values of $\mathcal{G}$ for arbitrary (l,m,n). Accuracy is quite important in order to faithfully calculate the effect of interference among the scattered wave components when many defects are present. Recall that the exact results can be expressed as an infinite perturbation series so that a modest error in phase in any iterated component could yield substantial spurious effects.

An iterative technique has recently been developed by Morita[7] in which a knowledge of the Greens function at the three sites (0, 0, 0), (2, 0, 0) and (3, 0, 0) can be used to generate values of $\mathcal{G}(\Omega;l,m,n)$ at any of the other lattice coordinates. We do not present Morita's complete arguments here, but rather quote the equations necessary to calculate the Greens function. In particular we point

out an error in one of the published expressions.

The recurrence relations that are used to connect the value of the Greens function at the sites (0, 0, 0), (2, 0, 0) and (3, 0, 0) to its value at other lattice sites is most easily written in a rotated system of coordinates. We rotate the angles x and y in (4.1) to x' and y' as follows:

$$x' = (x + y)/2 \quad ; \quad y' = (x - y)/2$$
$$l' = l + m \quad ; \quad m' = l - m \qquad (5.2)$$

so that the Greens function on the rotated system are

$$\mathcal{G}^1(\Omega;l',m',n) = \mathcal{G}(\Omega;\ (l' + m')/2,(l' - m')/2,n) \qquad (5.3a)$$

$$\mathcal{G}^1(\Omega;\ l+m,l-m,n) = \mathcal{G}(\Omega;l,m,n) \qquad (5.3b)$$

as can be verified by direct substitution into the integral (5.1). Note that l' and m' are either both even, or both odd integers.

Morita's scheme is based on the difference equation for the lattice Greens function restricted to the n=0 plane. The specific equation he obtains is

$$(m'+1)\left[\mathcal{G}^1(l'+2,m'+2,0) + 2\mathcal{G}^1(l',m'+2,0) + \mathcal{G}^1(l'-2,m'+2,0)\right]$$

$$-2(2m'+1)\,\Omega\left[\mathcal{G}^1(l'+1,m'+1,0) + \mathcal{G}^1(l'-1,m'+1,0)\right]$$

$$+ 2m'\left[\mathcal{G}^1(l'+2,m',0) + 2\Omega^2\,\mathcal{G}^1(l',m',0) + \mathcal{G}^1(l'-2,m',0)\right]$$

$$-2(2m'-1)\,\Omega\left[\mathcal{G}^1(l'+1,m'-1,0) + \mathcal{G}^1(l'-1,m'-1,0)\right]$$

$$+ (m'-1)\left[\mathcal{G}^1(l'+2,m'-2,0) + 2\mathcal{G}^1(l',m'-2,0) + \mathcal{G}^1(l'-2,m'-2,0)\right] = 0 \qquad (5.4)$$

The manipulation of (5.4) to create a recursion formula for $\mathcal{G}^1$ can be found in Moritas' paper. Figure (2) depicts a flow chart of the logic used in the computer program to obtain $\mathcal{G}^1$. The quantities A through F used in this procedure are:

$$A = p^{-1}\Big\{ (4p-1)\ \Omega\ \Big[\mathcal{G}^1(2p,2,0) + \mathcal{G}^1(2p,0,0)\Big]$$
$$-(2p-1)\ \Big[\mathcal{G}^1(2p-1,3,0) + (2\Omega^2+1)\ \mathcal{G}^1(2p-1,1,0)\ \Big]$$
$$+(4p-3)\ \Omega\ \Big[\mathcal{G}^1(2p-2,2,0) + \mathcal{G}^1(2p-2,0,0)\Big]$$
$$-(p-1)\ \Big[\mathcal{G}^1(2p-3,3,0) + 3\mathcal{G}^1(2p-3,1,0)\Big]\Big\} \qquad (5.5a)$$

$$B = \Omega\,[\,3\mathcal{G}^1(2p,2,0) + \mathcal{G}^1(2p,0,0)]$$
$$-2\,[\,\mathcal{G}^1(2p-1,3,0) + \Omega^2\,\mathcal{G}^1(2p-1,1,0)]$$
$$+\ \Omega[\,3\mathcal{G}^1(2p-2,2,0) + \mathcal{G}^1(2p-2,0,0)]$$
$$-[\mathcal{G}^1(2p-3,3,0) - \mathcal{G}^1(2p-3,1,0)]\ . \qquad (5.5b)$$

$$C = (m'+1)\,[2\mathcal{G}^1(l',m'+2,0) + \mathcal{G}^1(l'-2,m'+2,0)\,]$$
$$-2\Omega(2m'+1)\,[\mathcal{G}^1(l'+1,m'+1,0) + \mathcal{G}^1(l'-1,m'+1,0)]$$
$$+\ 2m'\,[\mathcal{G}^1(l'+2,m',0) + 2\Omega^2\,\mathcal{G}^1(l',m',0) + \mathcal{G}^1(l'-2,m',0)]$$
$$-2\Omega\,(2m'-1)\,[\mathcal{G}^1(l'+1,m'-1,0) + \mathcal{G}^1(l'-1,m'-1,0)]$$
$$+\ (m'-1)\,[\mathcal{G}^1(l'+2,m'-2,0) + 2\,\mathcal{G}^1(l',m'-2,0)] \qquad (5.5c)$$

$$D = (2p+1)^{-1}\Big\{2(4p+1)\Omega\mathcal{G}^1(2p+1,1,0)$$
$$-\ 4p[\,\mathcal{G}^1(2p,2,0) + \Omega^2\mathcal{G}^1(2p,0,0)\,]$$
$$+\ 2\,(4p-1)\Omega\ \mathcal{G}^1(2p-1,1,0)$$
$$-(2p-1)\,[\mathcal{G}^1(2p-2,2,0) + \mathcal{G}^1(2p-2,0,0)]\Big\} \qquad (5.5d)$$

$$E = 2\Omega\,[\,5\,\mathcal{G}^1(2p+1,3,0) + 3\mathcal{G}^1(2p+1,1,0)]$$
$$-\ 6\,\mathcal{G}^1(2p,4,0) - 8\Omega^2\,\mathcal{G}^1(2p,2,0) - 2\,\mathcal{G}^1(2p,0,0)$$

$$+ 2\Omega[5\,\mathcal{G}^1(2p-1,3,0) + 3\,\mathcal{G}^1(2p-1,1,0)]$$

$$- 3\,\mathcal{G}^1(2p-2,4,0) - 4\,\mathcal{G}^1(2p-2,2,0) - \mathcal{G}^1(2p-2,0,0) \qquad (5.5e)$$

$$F = 2\Omega\,[(4+p)\,\mathcal{G}^1(2p+1,3,0) + (2-p)\,\mathcal{G}^1(2p+1,1,0)]$$

$$- 3\,\mathcal{G}^1(2p,4,0) - 4\,(\Omega^2(p+1)+1)\,\mathcal{G}^1(2p,2,0) + (4p\,\Omega^2-1)\,\mathcal{G}^1(2p,0,0)$$

$$+ 2\Omega\,[(1+p)\,\mathcal{G}^1(2p-1,3,0) + (1-p)\,\mathcal{G}^1(2p-1,1,0)] \qquad (5.5f)$$

Equations (5.5a) - (5.5c) inclusive, correspond to Eqs. (5.7), (5.4) (5.9b) and (5.10b) of Morita respectively. However, Moritas' Eq. (5.12b) is incorrect and (5.5e) takes its place.

Finally, to calculate values of $\mathcal{G}^1(l',m',n)$ for nonzero n (and hence $\mathcal{G}(l,m,n)$ also), we use a modification of equations (5.3)and (5.4) of Morita namely

$$\mathcal{G}^1(l',m',1) = \Omega\,\mathcal{G}^1(l',m',0) - \frac{1}{2}\mathcal{G}^1(l+1,m'+1,0) + \mathcal{G}^1(l'+1,m'-1,0) + \mathcal{G}^1(l'-1,m'+1,0) - \frac{1}{2}\,\mathcal{G}^1(l'-1,m'-1,0) \qquad (5.6)$$

and, for $n \geq 2$,

$$\mathcal{G}^1(l',m',n) = 2\Omega\,\mathcal{G}^1(l',m',n-1) - \mathcal{G}^1(l',m',n-2) - \mathcal{G}^1(l'+1,m'+1,n-1) - \mathcal{G}^1(l'-1,m'-1,n-1) - \mathcal{G}^1(l'+1,m'-1,n-1) - \mathcal{G}^1(l'-1,m'+1,n-1) \qquad (5.7)$$

Before the above recursion scheme can be applied, however, we require $\mathcal{G}(0,0,0)$, $\mathcal{G}(2,0,0)$ and $\mathcal{G}(3,0,0)$ ($\mathcal{G}^1(0,0,0)$, $\mathcal{G}^1(2,2,0)$ and $\mathcal{G}^1(3,3,0)$) as input.

The simple cubic lattice Greens function $\mathcal{G}(\Omega\,;\,1,\,0,\,0)$ has a convenient representation in terms of complete elliptic integrals of the first kind.[8] The Greens function is pure real for $3 \geq \Omega$, and is given by

$$\mathcal{G}(\Omega \geq 3;l,0,0) = \frac{1}{\pi^2}\int_0^{\pi} d\Theta\,\cos(l\,\Theta)\kappa K(\kappa) \qquad (5.8)$$

where $\kappa \equiv 2(\Omega - \cos\Theta)^{-1}$ is the parameter of the complete elliptic integral

$$K(\kappa) \equiv \int_0^{\pi/2} \frac{d\Theta}{\sqrt{1 - \kappa^2 \sin^2\Theta}} \quad . \tag{5.9}$$

For $1 \leq \Omega \leq 3$, one has for the real and imaginary parts of the Greens function

$$\mathcal{G}^R(\Omega;l,0,0) = \frac{1}{\pi^2} \int_0^{\cos^{-1}(\Omega-2)} d\Theta \cos(l\Theta)\, K(\kappa_1)$$

$$+ \frac{1}{\pi^2} \int_{\cos^{-1}(\Omega-2)}^{\pi} d\Theta \cos(l\Theta) K(\kappa) \tag{5.10}$$

$$\mathcal{G}^I(\Omega;l,0,0) = \frac{1}{\pi^2} \int_0^{\cos^{-1}(\Omega-2)} d\Theta \cos(l\Theta)\, K(\kappa'_1) \tag{5.11}$$

where

$$\kappa_1 = \kappa^{-1} \text{ and } \kappa_1' = \sqrt{1 - \kappa_1^2} \quad . \tag{5.12}$$

In the range $0 \leq \Omega \leq 1$, we have

$$\mathcal{G}^R(\Omega;l,0,0) = -\frac{1}{\pi^2} \int_0^{\cos^{-1}\Omega} d\Theta \cos(l\Theta) K(\kappa_1) + \frac{1}{\pi^2} \int_{\cos^{-1}\Omega}^{\pi} d\Theta \cos(l\Theta) K(\kappa_1) \tag{5.13}$$

$$\mathcal{G}^I(\Omega;l,0,0) = \frac{1}{\pi^2} \int_0^{\pi} d\Theta \cos(l\Theta)\, K(\kappa_1') \tag{5.14}$$

where κ_1 and κ_1' are given in (5.12). Formulas (5.8) - (5.14) were numerically evaluated for $l = 0$, 2 and 3 and used as input for the recursion scheme previously described. Figure 3 shows plots of the real and imaginary parts of $\mathcal{G}(\Omega;0,0,0)$, $\mathcal{G}(\Omega;2,0,0)$ and $\mathcal{G}(\Omega;3,0,0)$.

6. RESULTS OF SCATTERING CALCULATIONS

In this section we present some results of scattering plane waves off various planar configurations of point scatterers. We have chosen the incident radiation to have wavelength equal to the lattice spacing b, and to propagate in the $\hat{z}$ direction. All scatterers lie in the perpendicular x-y plane. Polar angles Θ, φ define the directions along which we view the scattering amplitude $f(\Theta, \varphi)$ (see figure 4).

A. Scattering From a Line.

The first sequence of numerical results we show are polar perspective plots of the magnitude $|f(\Theta,\varphi)|$ for one, two, three, four and five scatterers arranged to form a line. If just a single scattering center is present (located at the origin (0, 0, 0), say), there are no preferred directions for the scattering, therefore $|f|$ is uniform over all angles Θ,φ . The result of adding a second scattered at (1, 0, 0) is shown in Figure 5a. (The number and position of the scatterers is indicated in the upper left hand corner of the figure.) We see that the scattering amplitude in maximal in all directions perpendicular to the preferred axis, i.e. along $\varphi = \pi/2$ and $3\pi/2$ for all Θ values. $|f|$ is also maximal parallel to the x-axis, at $\varphi = 0, \pi$ and $\Theta = \pi/2$. The amplitude decreases away from these directions due to destructive interference among ray paths. The addition of a third scatterer, at (2, 0, 0), gives rise to Figure 5b. The directions of maximal $|f|$ remains the same (serving to identify the line of scatterers), but $|f|$ decreases more rapidly away from these regions than for the case of two scatterers. More significantly, a subsidiary ridge has appeared as a new topographic feature, marking the influence of multiple scattering events. Figures 5c and 5d show the effect of adding a fourth and a fifth defect. We see a further sharpening of the main ridges, and the introduction of additional subsidiary ridges.

B. Scattering from Perpendicular Lines

Figures 6a - 6d show a sequence of plots of $|f(\Theta,\varphi)|$ as we add to the line, but now in a perpendicular direction. This sequence is most easily understood if we first consider the scattering off a line of defects arranged along the y-axis (instead of the arrangement along the x-axis which led to Figure 5d). Symmetry implies that such an arrangement should lead to a scattering amplitude $f(\Theta, \varphi)$ related to the previous amplitude by the rotation $\Theta, \varphi \rightarrow \Theta, \varphi + \pi/2$. All features of the perspective plot of $|f|$ would simply be shifted by $\pi/2$ along the φ - axis. Bearing this in mind, the depression along the ridges at $\varphi = \pi/2, 3\pi/2$ in figure 6a and subsequent plots is understood as a combination of Figures 5d with the shifted versions of 5b - 5e. The configuration of scatterers which gave rise to Figure 6d has a symmetry line along $\varphi = \pi/4$, and we clearly see their symmetry in the scattering amplitude plot. The sequence of Figures 6a - 6d is a progression toward this symmetric arrangement.

C. Scattering From a Plane.

We now consider adding parallel lines of scatterers so as to form a plane square made out of twenty five scatterers. Figures 7a - 7d show the relevant sequence of plots. It helps to realize that the final square configuration (producing Figure 7d) is symmetric around $\varphi = 0, \pi/4$ and $\pi/2$. The sequence of Figures 7a - 7d shows progression toward the symmetric result.

D. Scattering From a Cavity.

Finally, we consider scattering from cavities obtained from the square configuration of Figure 7d by removing scatterers from the interior. Comparing Figures 7d and 8c it is apparent that there is significantly more structure in the cross section for scattering from a cavity than for scattering from the rectangle. The increased multiple scattering effects in the cavity enhance the subsidiary maxima at $\Theta = \pi/4, \pi/2$ and $3\pi/2$.

REFERENCES

1. E.W. Montroll and B.J. West, J. Stat. Phys. **13**, 17 (1975). B.J. West, Am. J. Phys. **46**, 1236 (1978).

2. see eg. V. Frisch, in *Probability Methods in Applied Mathematics*, edited by A.T. Bharucha-Reid (Academic Press, New York, 1968).

3. see eg. H.C. van de Hulst, *Light Scattering by Small Particles*, Dover Pub. New York, (1957, 1981).

4. P.M. Morse and K.U. Ingard, *Theoretical Acoustics*, McGraw-Hill, New York (1968).

5. J.E. Gubernatis, J.A. Krumhansel and R.M. Thomson, J. Appl. Phys. **50**, 3338 (1979).

6. J.B. Keller, J. Opt. Soc. of Am. **52**, 116 (1962).

7. T. Morita, J. Phys. A: Math. Gen. **8**, 478 (1975).

8. T. Horiguchi, J. Phys. Soc. Japan **30**, 1261 (1971).

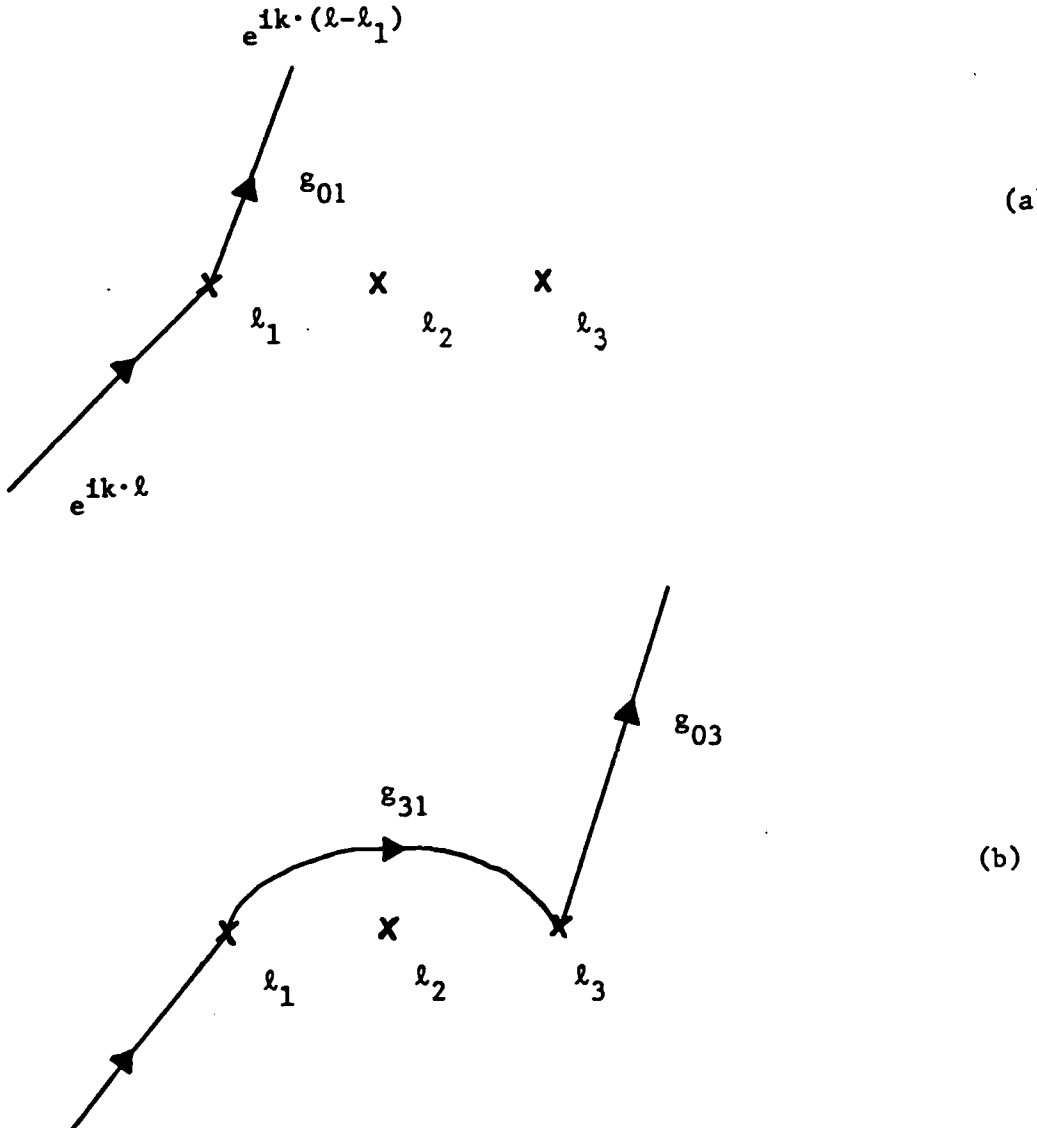

Figure 1. (a) Single scattering of plane wave by potential at site l_1.
(b) Double scattering of plane wave from lattice site l, to lattice site l_3, followed by scattering from l_3 to observer.

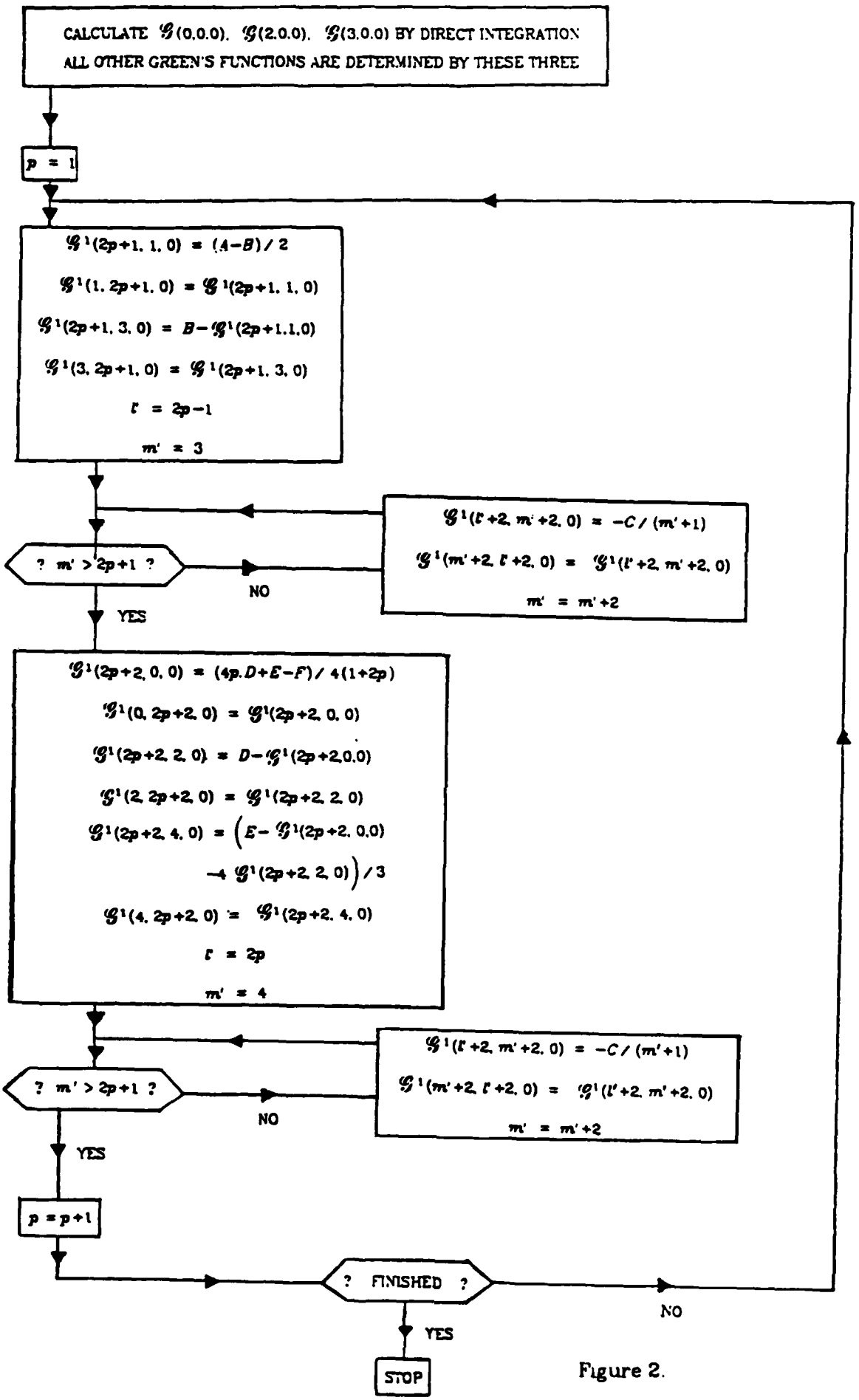
CALCULATE $\mathcal{G}(0,0,0)$, $\mathcal{G}(2,0,0)$, $\mathcal{G}(3,0,0)$ BY DIRECT INTEGRATION
ALL OTHER GREEN'S FUNCTIONS ARE DETERMINED BY THESE THREE
$p = 1$
$\mathcal{G}^1(2p+1, 1, 0) = (A-B)/2$
$\mathcal{G}^1(1, 2p+1, 0) = \mathcal{G}^1(2p+1, 1, 0)$
$\mathcal{G}^1(2p+1, 3, 0) = B - \mathcal{G}^1(2p+1, 1, 0)$
$\mathcal{G}^1(3, 2p+1, 0) = \mathcal{G}^1(2p+1, 3, 0)$
$\ell = 2p-1$
$m' = 3$
? $m' > 2p+1$?
NO
$\mathcal{G}^1(\ell+2, m'+2, 0) = -C/(m'+1)$
$\mathcal{G}^1(m'+2, \ell+2, 0) = \mathcal{G}^1(\ell+2, m'+2, 0)$
$m' = m'+2$
YES
$\mathcal{G}^1(2p+2, 0, 0) = (4p \cdot D + E - F)/4(1+2p)$
$\mathcal{G}^1(0, 2p+2, 0) = \mathcal{G}^1(2p+2, 0, 0)$
$\mathcal{G}^1(2p+2, 2, 0) = D - \mathcal{G}^1(2p+2, 0, 0)$
$\mathcal{G}^1(2, 2p+2, 0) = \mathcal{G}^1(2p+2, 2, 0)$
$\mathcal{G}^1(2p+2, 4, 0) = \left(E - \mathcal{G}^1(2p+2, 0, 0) - 4\,\mathcal{G}^1(2p+2, 2, 0)\right)/3$
$\mathcal{G}^1(4, 2p+2, 0) = \mathcal{G}^1(2p+2, 4, 0)$
$\ell = 2p$
$m' = 4$
? $m' > 2p+1$?
NO
$\mathcal{G}^1(\ell+2, m'+2, 0) = -C/(m'+1)$
$\mathcal{G}^1(m'+2, \ell+2, 0) = \mathcal{G}^1(\ell+2, m'+2, 0)$
$m' = m'+2$
YES
$p = p+1$
? FINISHED ?
NO
YES
STOP

Figure 2.

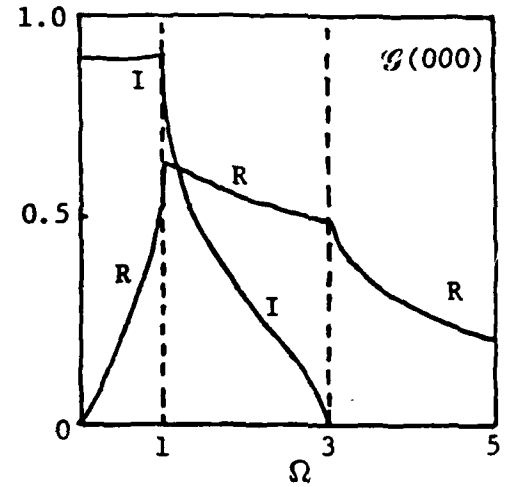

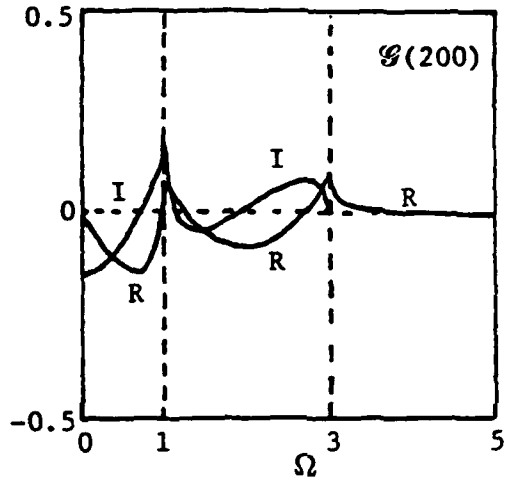

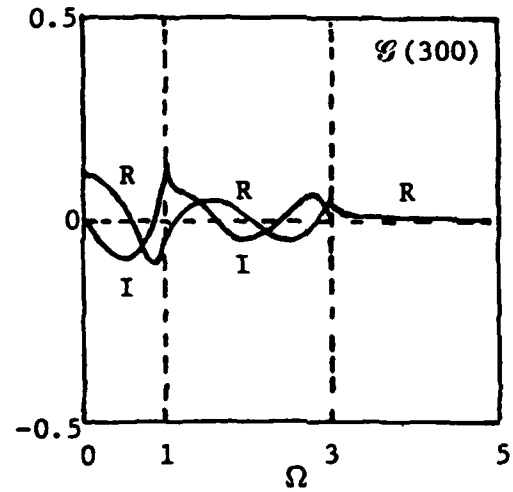

Figure 3. Real and imaginary parts of S.C. Green's functions $\mathcal{G}(0, 0, 0)$, $\mathcal{G}(2, 0, 0)$, and $\mathcal{G}(3, 0, 0)$. These are used as input for Morita's recursion scheme.

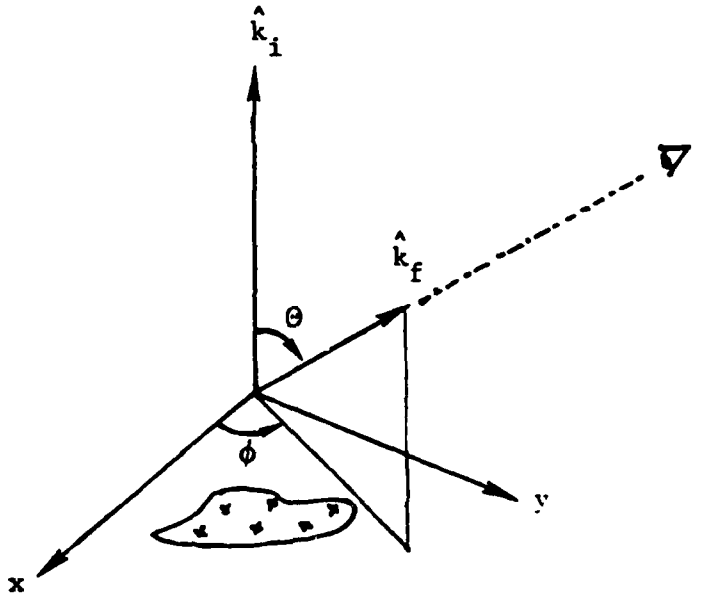

Figure 4. Polar angles Θ, φ for viewing scattering amplitude $f(\Theta,\varphi)$.

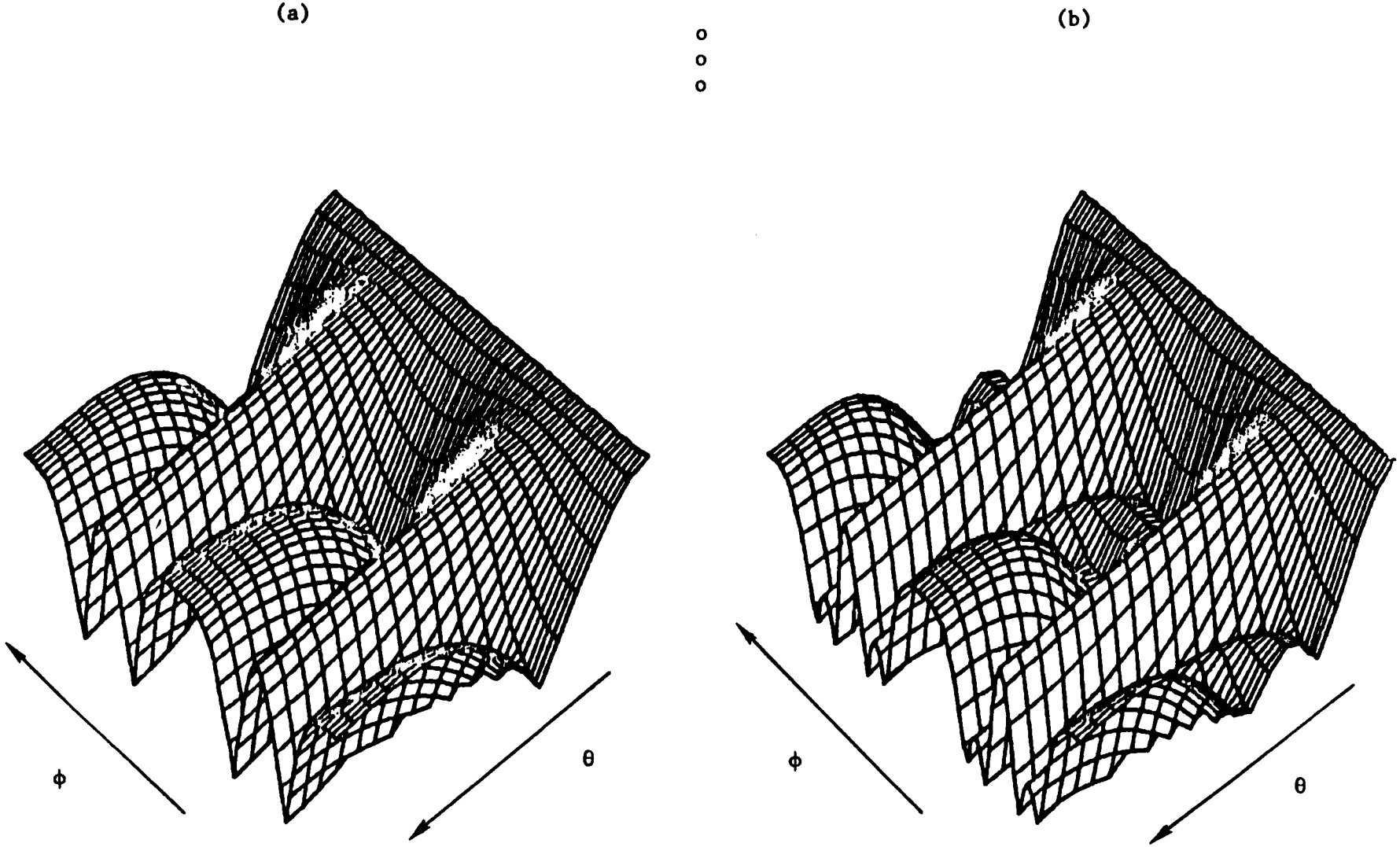

Figure 5. Polar perspective plot of $|f(\theta\varphi)|$ for scattering from n point scatterers in a line with maximum amplitude $|f_{max}|$: (a) n = 2, $|f_{max}| \simeq 64$; (b) n = 3, $|f_{max}| \simeq 92$.

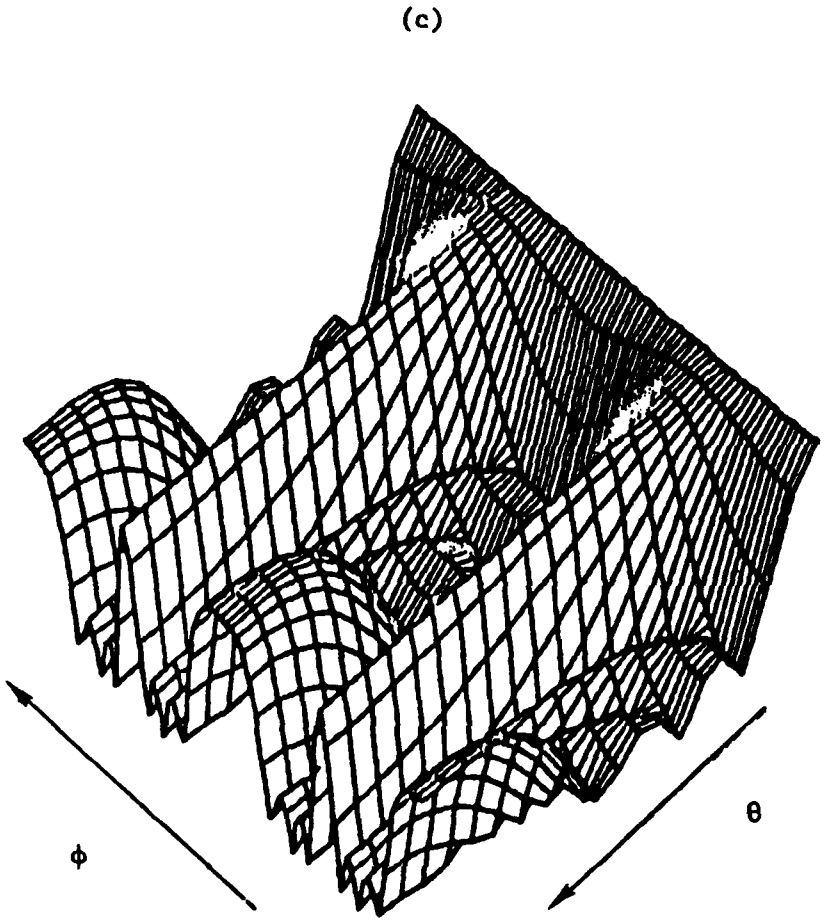

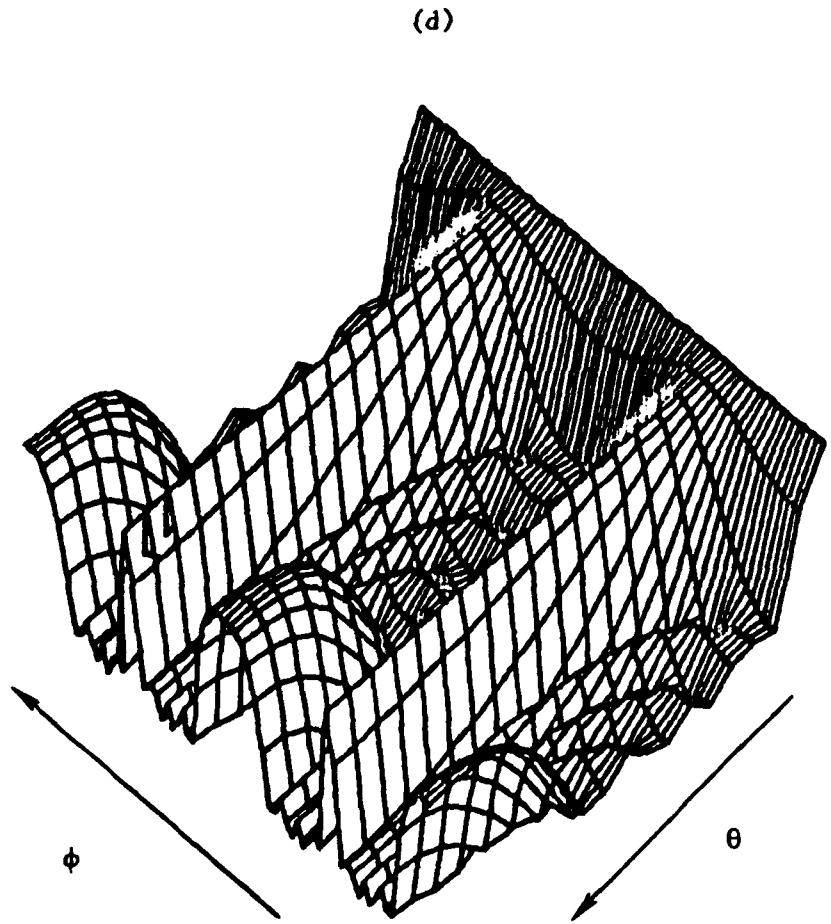

Figure 5 (continued): (c) n = 4, $|f_{max}| \simeq 119$ and (d) n = 5, $|f_{max}| \simeq 146$.

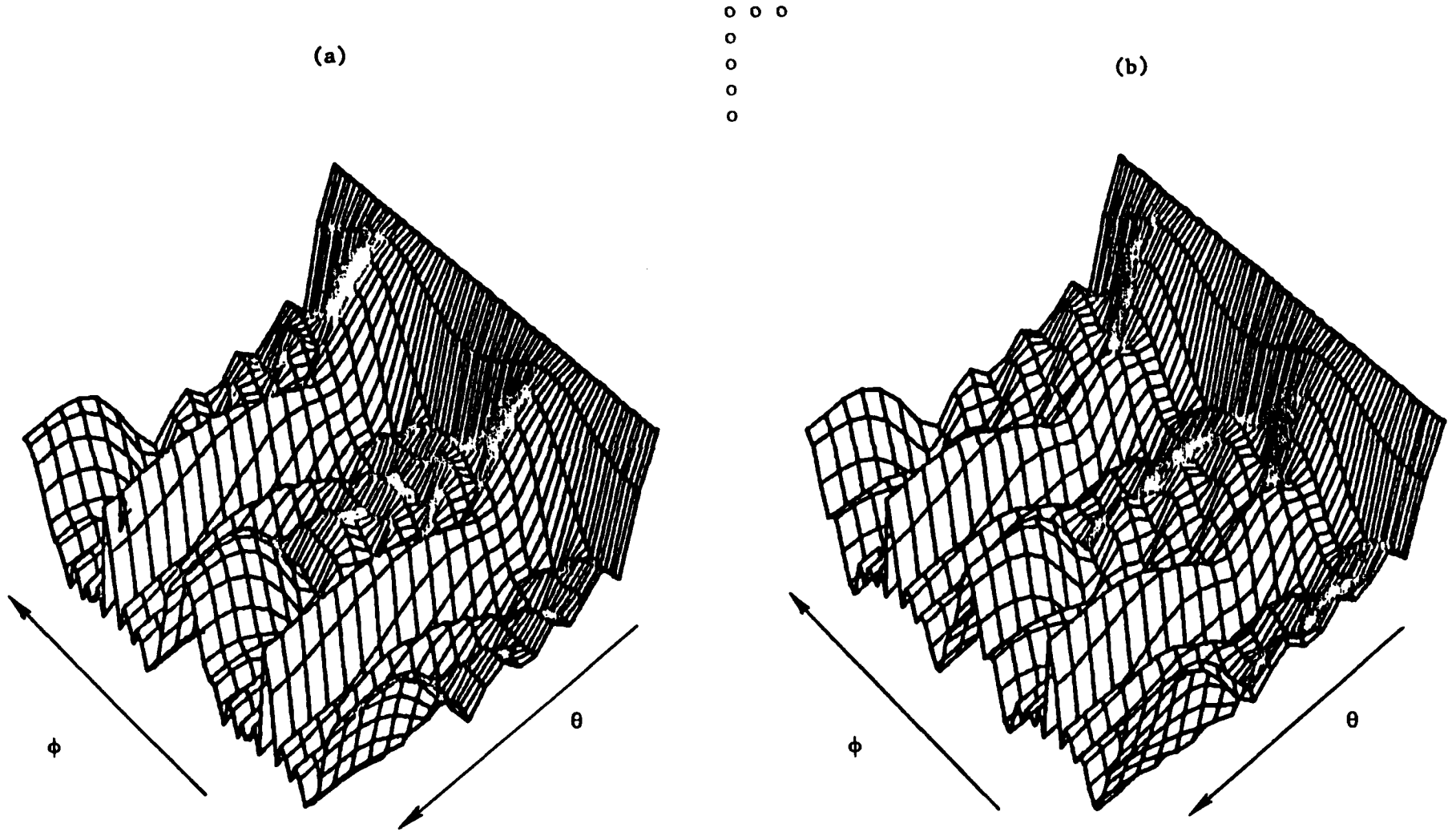

Figure 6. Polar perspective plots of $|f(\Theta,\varphi)|$ for scattering from 5 point scatterers along the x-axis and n-point scatterers along the y-axis; $|f_{max}|$ is the maximum amplitude of the scattered wave: (a) n = 2, $|f_{max}| \simeq 216$; (b) n = 3 , $|f_{max}| \simeq 135$.

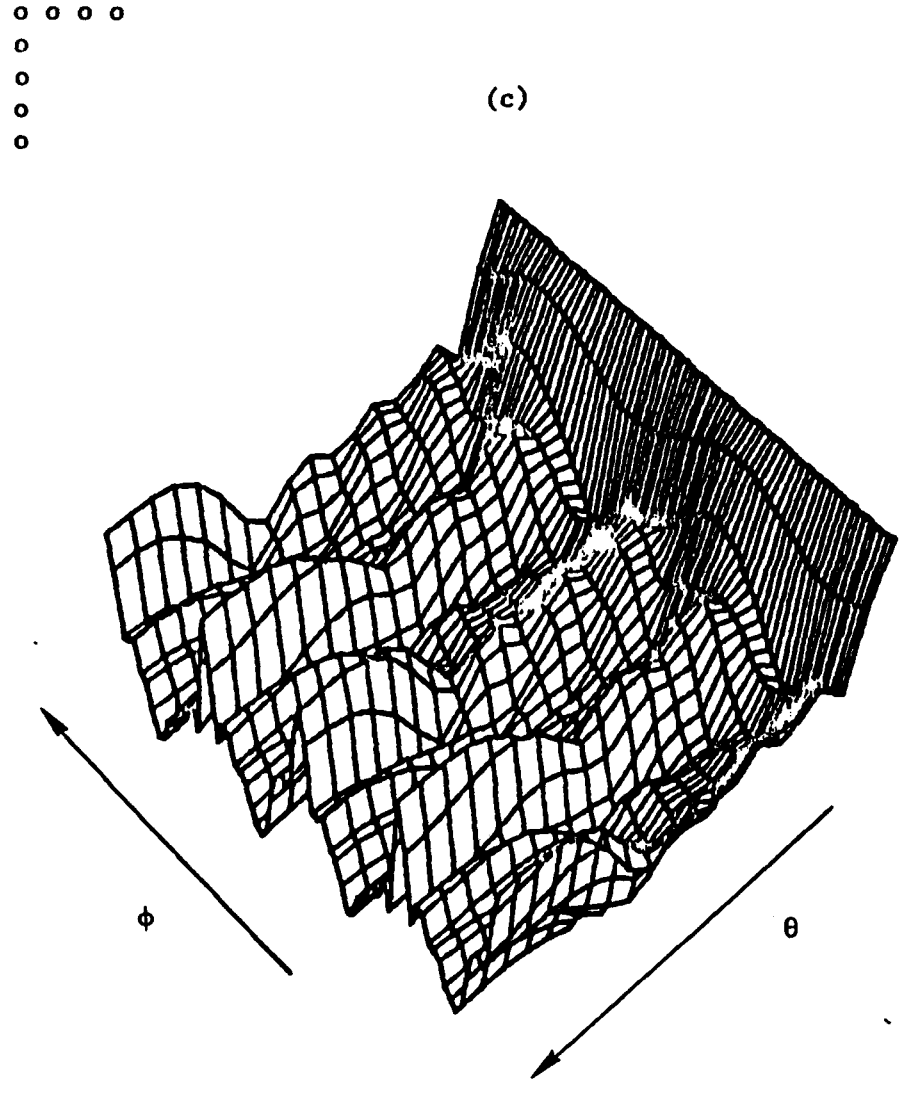

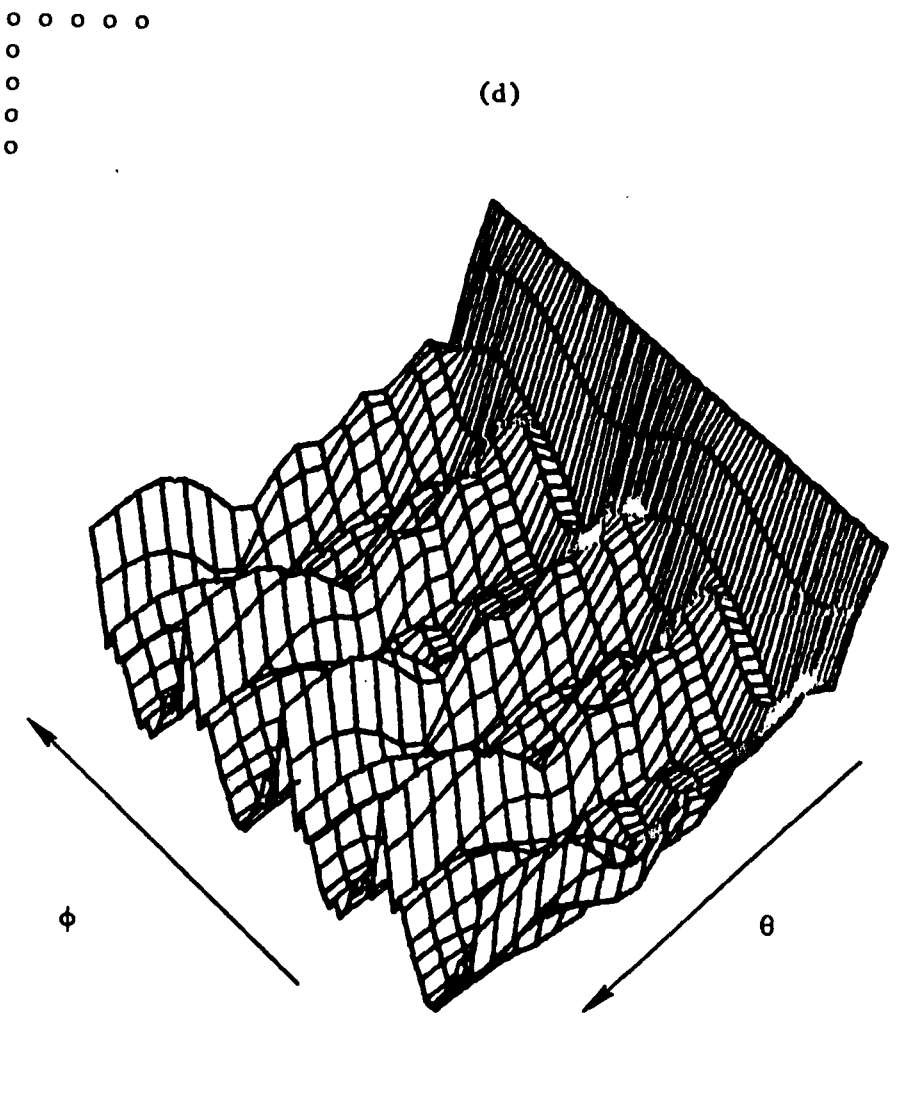

Figure 6 (continued). (c) n = 4 , $|f_{max}| \simeq 168$; (d) n = 5 , $|f_{max}| \simeq 165$.

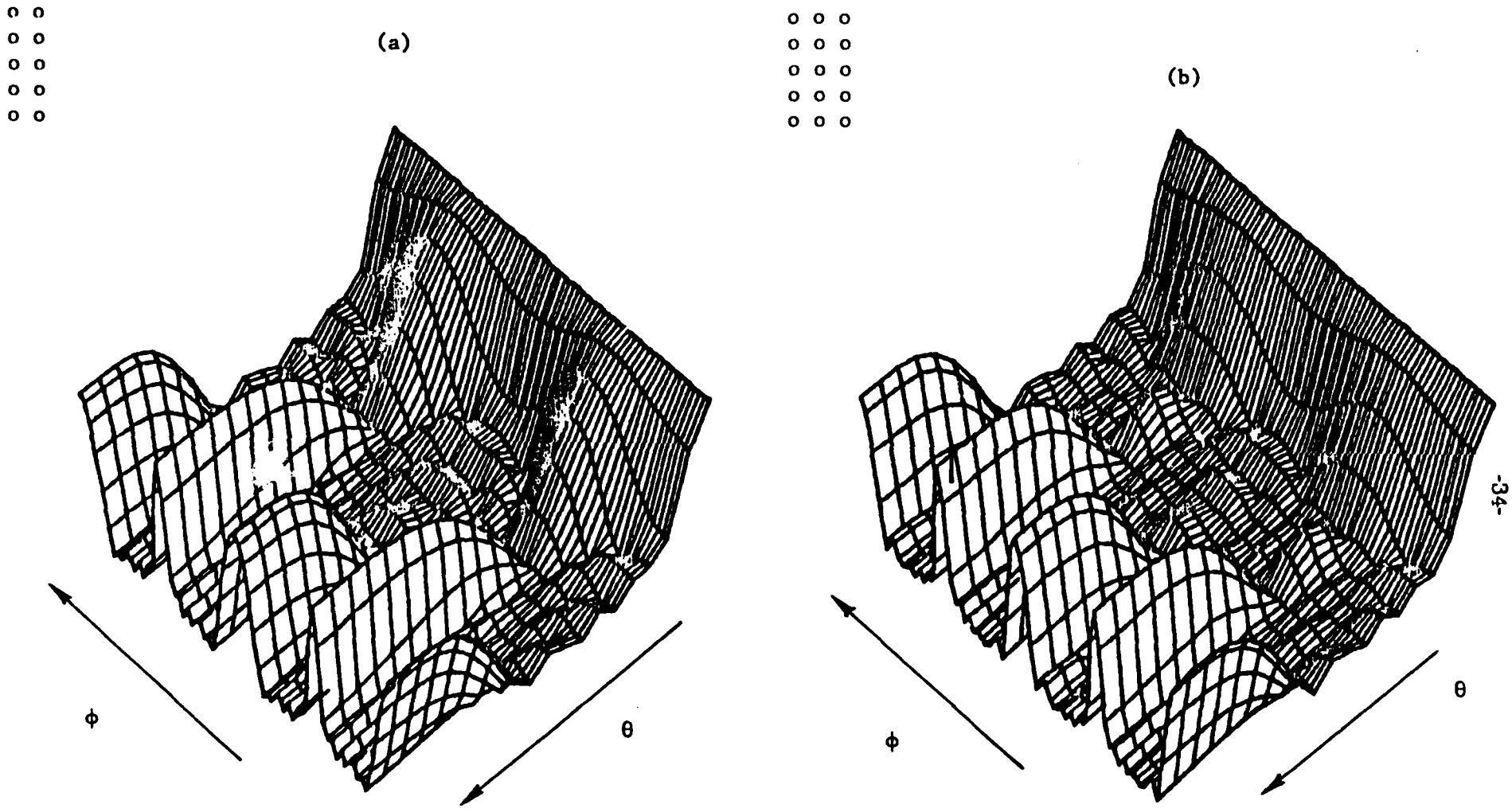

Figure 7. Polar perspective plots of $|f(\theta,\varphi)|$ for scattering from n rows of 5 point scatterers each and $|f_{max}|$ is the maximum scattering amplitude: (a) n = 2, $|f_{max}| \simeq 310$; (b) n = 3, $|f_{max}| \simeq 262$.

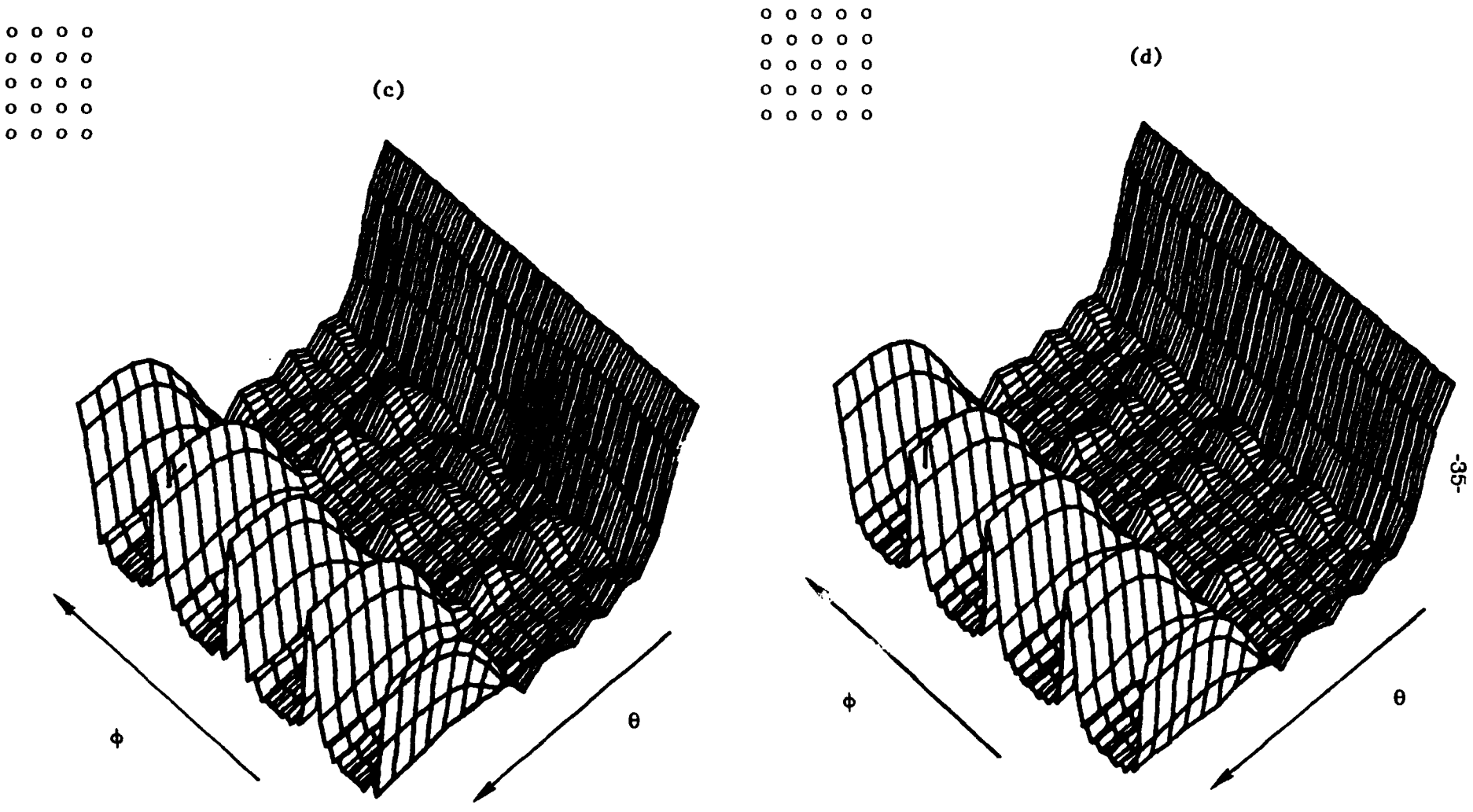

Figure 7 (continued). (c) $n = 4$, $|f_{max}| \simeq 391$; (d) $n = 5$, $|f_{max}| \simeq 575$.

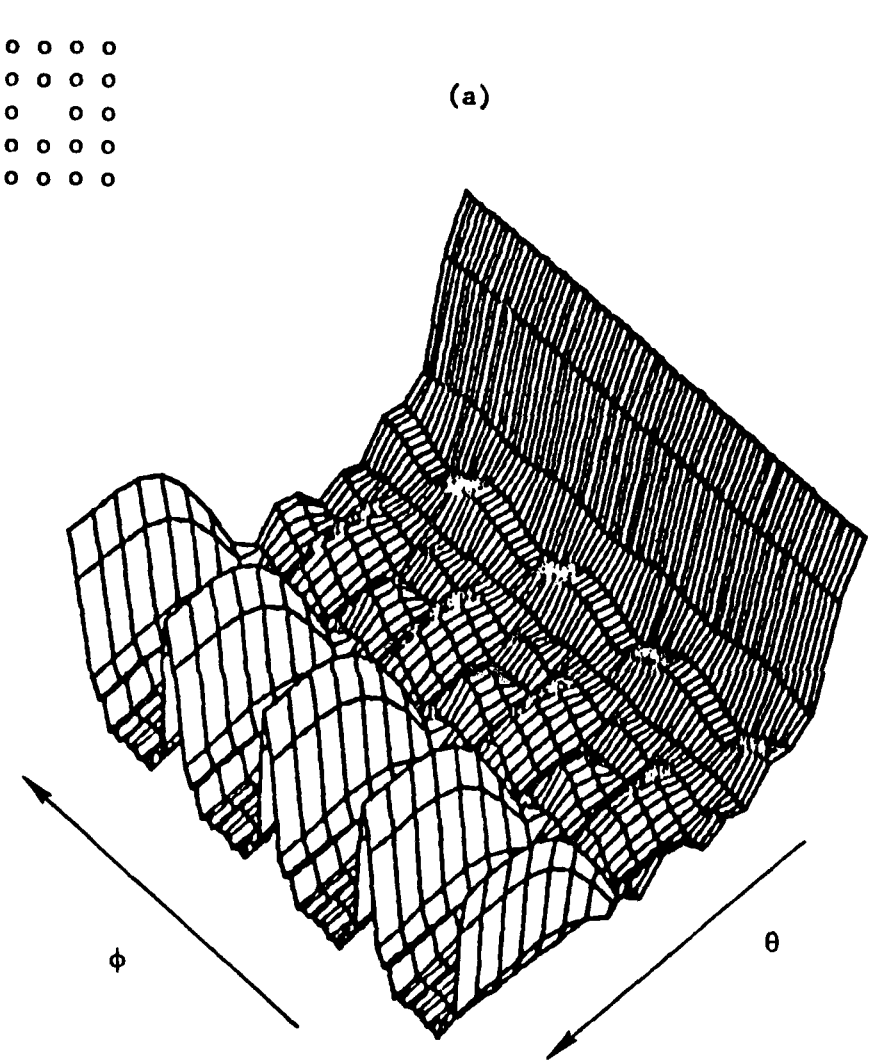

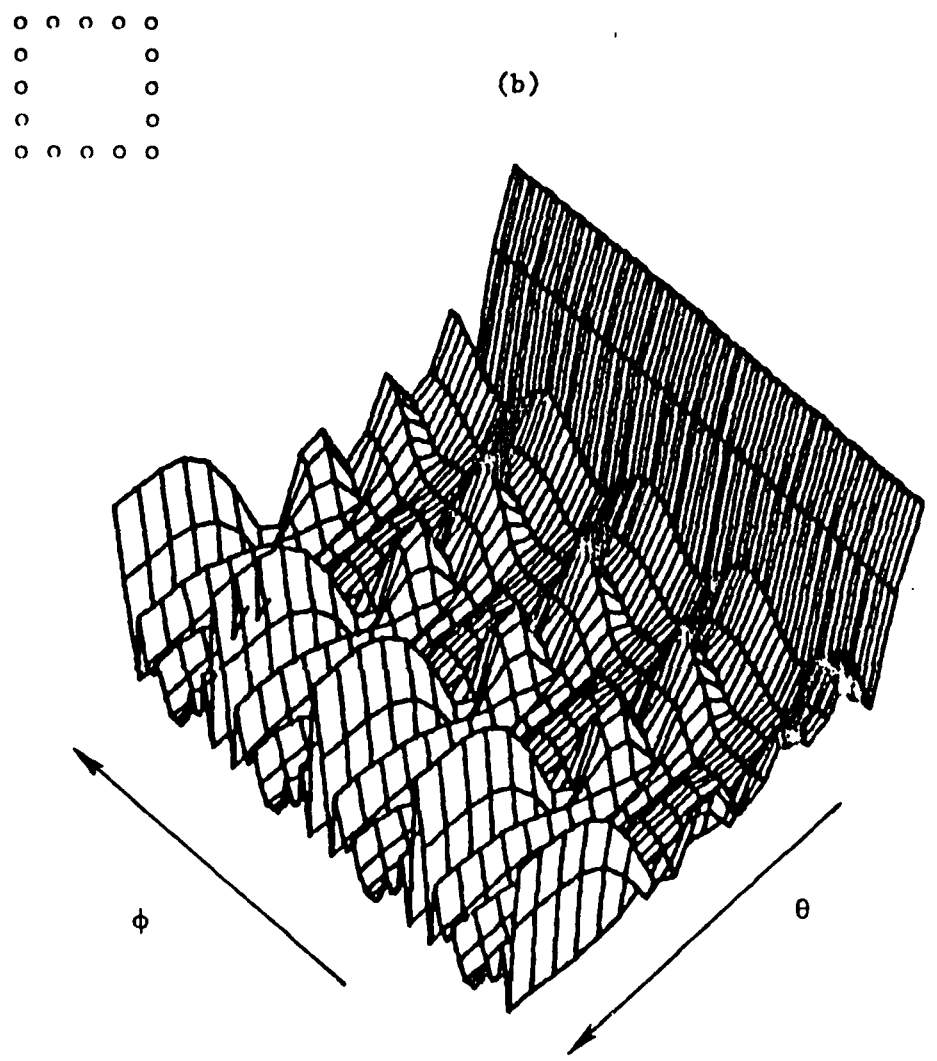

Figure 8. Polar perspective plots of $|f(\theta,\varphi)|$ for scattering from 5 x 5 square of point scatterers. In (a) the center scatterer is absent and $|f_{max}| \simeq 566$. In (b) only the scatterers on the perimeter are kept and $|f_{max}| \simeq 445$.

END

FILMED

9-83

DTIC